



Research



Cite this article: Tarnovsky YC, Sheinin A, Laufer A, Yovel Y. 2026 In-flight brainstem responses highlight the encoding of self-emitted echolocation calls in bats. *Proc. R. Soc. B* **293**: 20252988.

<https://doi.org/10.1098/rspb.2025.2988>

Received: 19 November 2025

Accepted: 12 January 2026

Subject Category:

Neuroscience and cognition

Subject Area:

neuroscience

Keywords:

bats, echolocation, active sensing, auditory brainstem response

Author for correspondence:

Yossi Yovel

e-mail: yossiyovel@gmail.com

Electronic supplementary material is available online at <https://doi.org/10.6084/m9.figshare.c.8259589>.

In-flight brainstem responses highlight the encoding of self-emitted echolocation calls in bats

Yifat Chaya Tarnovsky^{1,2}, Anton Sheinin³, Aharon Laufer² and Yossi Yovel^{2,3}

¹School of Neurobiology, Biochemistry and Biophysics, ²School of Zoology, and ³Sagol School of Neuroscience, Tel Aviv University, Tel Aviv, Israel

YCT, 0009-0008-2903-1616; YY, 0000-0001-5429-9245

Echolocating bats rely on precise auditory processing to navigate and forage in complete darkness. A critical aspect of this behaviour is the neural encoding of self-generated vocalizations, which allows for accurate comparison with returning echoes. In this study, we introduce a non-invasive method for recording auditory brainstem responses (ABRs) in awake, flying big brown bats (*Eptesicus fuscus*). Using a custom 3D-printed harness that enables sustained in-place flight, we simultaneously recorded electroencephalographic and acoustic signals from freely vocalizing animals. Self-emitted echolocation calls reliably evoked ABRs, including a distinct pre-auditory wave that occurred before call onset and is probably associated with motor command generation. We were able to extract single-trial individual ABR patterns, which revealed significant correlations between specific acoustic properties of the calls and both ABR amplitude and latency. These findings demonstrate that, despite the suggested peripheral attenuation of self-emitted echolocation calls, the bat auditory system dynamically encodes the characteristics of outgoing vocalizations, with information extraction occurring as early as the brainstem. Our approach offers an effective framework for investigating sensory–motor integration in actively behaving animals.

1. Introduction

Echolocating bats are auditory specialists capable of foraging in darkness by actively emitting acoustic signals and analysing the returning echoes from objects in their environment [1,2]. Bats dynamically adapt the design of their echolocation calls in response to changes in the acoustic scene [3,4]. Because echolocation depends on comparing emitted signals with returning echoes, an accurate neural representation of the self-emitted calls is essential [5–7].

Several mechanisms have been proposed to explain how bats register the characteristics of their emitted signals. One of the most prominent ones is that they monitor their own vocalizations via auditory feedback [6]. Unlike other mechanisms—such as relying on a neural efference copy—listening to the emitted sound has the advantage of capturing its actual acoustic properties, rather than merely the motor plan for producing it.

Here, we examined whether the properties of emitted echolocation signals are encoded in the auditory brainstem response (ABR). The ABR is an evoked neural response generated by synchronous activity in the early stages of auditory processing. Wave I of the ABR reflects the compound response of the auditory nerve, while later waves correspond to activity in successive nuclei of the ascending auditory pathway: the cochlear nucleus, the superior olivary complex, the nucleus of the lateral lemniscus and the inferior colliculus [8,9].

Most ABR recordings in bats to date have been conducted under anaesthesia, which might alter physiological function, affecting both central and

peripheral components of auditory processing [10]. These effects have been shown to modify ABR characteristics across a variety of vertebrate species, including mice, rats, birds, lizards and frogs [11]. Moreover, working with anaesthetized bats limits the ability to investigate the ABR representation of echolocation calls emitted by the bat as part of its natural active-sensing processes.

Simmons *et al.* [12] demonstrated the feasibility of non-invasive scalp recordings of auditory-evoked activity in awake, unrestrained big brown bats. However, their method required that the animals be trained to remain motionless, limiting its applicability to study flying echolocating bats. To overcome this challenge, we developed a system for recording ABRs non-invasively in awake, behaving big brown bats (*Eptesicus fuscus*). The small body size of most bat species poses a challenge for equipping them with high-end on-board recording systems that still allow them to fly (but see [13]). We designed a custom 3D-printed harness that allowed bats to fly in place and echolocate without forward progression, while remaining connected to non-invasive surface electrodes. We used this method to record the ABR representation of echolocation calls and showed how key acoustic parameters of the calls are encoded in the auditory brainstem.

Our recordings revealed that self-emitted echolocation calls evoke ABRs during flight, including a distinct pre-auditory wave (PAW) that preceded call onset, probably reflecting motor generation commands. Individual-trial analyses showed that ABR amplitudes in waves II and III increased systematically with both call duration and intensity, whereas wave I showed no such interaction, suggesting progressive integration of acoustic features along the brainstem. Additionally, ABR latencies were positively correlated with call duration across all waves. Together, these results demonstrate that the bat auditory system encodes the detailed acoustic structure of self-generated vocalizations at the level of the brainstem, providing a neural substrate for rapid sensory–motor coordination during echolocation.

2. Results

(a) Auditory brainstem response recordings

Neural responses to self-emitted biosonar echolocation calls were recorded from three big brown bats (*E. fuscus*) while flying in place within a sound-attenuated Faraday cage (figure 1A; electronic supplementary material, video S1). The bats were secured in a custom harness, allowing natural echolocation during restrained flight. Synchronized electroencephalographic (EEG) signals were recorded non-invasively in parallel to acoustic recordings (figure 1B).

For bat #3, two control recordings were obtained: (i) EEG recorded during passive listening to a playback of the same bat's own echolocation calls while the bat was awake and restrained; and (ii) EEG recorded during flight in the harness with electrodes placed on the lower back, where no neural signal is expected.

All three bats exhibited ABRs to their own calls during flight (figure 2A) and during control playback (figure 2B). The control recording with electrodes placed on the back during flight showed no response (figure 2C), confirming the neural origin of the ABR signal. Notably, in all bats, the ABRs were prefaced with a distinct electrophysiological potential that started 0–5 ms prior to call arrival at the ears, unlike during passive hearing when activation started approximately 2 ms after the sound's arrival at the ears (figure 2; compare ABRs in panels A and B). This potential is consistent with a PAW previously reported in echolocating dolphins [14,15].

(b) Individual auditory brainstem responses and acoustic correlates

Despite typical reliance on averaging to extract ABRs, we observed consistent response patterns in single trials. This allowed us to investigate individual ABRs (iABRs) as a function of acoustic echolocation call properties (figure 3).

To investigate whether acoustic call parameters are encoded by the ABR in echolocating bats, we modelled ABR latencies and amplitudes of waves I, II and III, which showed the highest signal-to-noise ratios (SNRs), as a function of echolocation call duration and intensity, while accounting for inter-individual variability. We used linear mixed-effect (LME) models, with call duration and intensity set as fixed factors, and bat ID and EEG trial noise included as random effects (see §4).

In waves II and III, a positive interaction between call duration and intensity and the ABR's log-amplitude was observed, indicating that the ABR peak amplitudes increased when echolocation calls were both longer and more intense (figure 4A; see table 1 for full model statistics).

The effect size of this interaction strengthened with wave number—from wave I, which showed no interaction ($\beta = 0.0003$), to wave II ($\beta = 0.004$), and peaking in wave III ($\beta = 0.005$; figure 4B).

The latency of the three ABR waves also revealed significant correlations with call acoustics, particularly call duration. Call duration was positively correlated with ABR latency in all three waves (figure 4C). We ran several analyses to ensure that this was not an artefact of call duration estimations (see details in electronic supplementary materials, figure S1 and table S1).

Random intercepts for bat ID accounted for meaningful between-subject variability across all models. EEG noise, included as a second random effect in the amplitude models, explained substantial additional variance related to the recording conditions.

3. Discussion

Echolocating bats actively probe their environment by emitting sound and analysing the returning echoes to construct a neural representation of their surroundings [2,16].

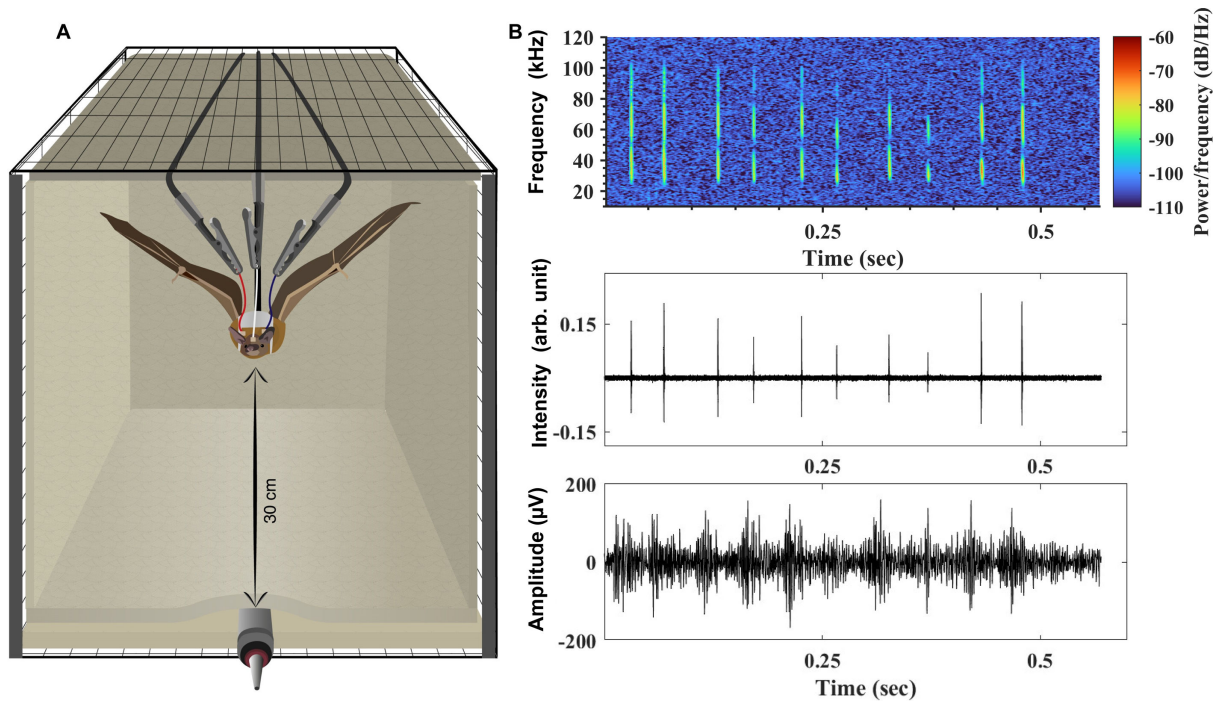


Figure 1. Experimental set-up. (A) Illustration of a bat in flight within the harness inside the Faraday cage. The microphone is positioned below, and EEG electrodes are placed above the animal's head. (B) A representative 0.5 s trace from bat #2 showing (top) spectrogram of the echolocation calls, (middle) waveform of the emitted calls and (bottom) synchronized EEG trace.

The small body size of most bat species poses a challenge for equipping them with on-board recording systems that still allow them to fly. Moreover, such systems often have reduced capabilities compared to full laboratory set-ups, including limited synchronization between auditory and EEG channels and a dynamic range insufficient for reliable ABR recordings. To overcome this challenge, we designed a custom 3D-printed harness that allowed big brown bats to fly in place and echolocate without forward progression, while remaining connected to non-invasive surface electrodes.

Echolocating bats dynamically modulate call duration during different phases of the hunting sequence, producing shorter calls as they approach their target or background objects [17,18]. This behaviour is widely interpreted as a strategy to avoid temporal overlap between emitted calls and returning echoes from nearby objects [19]. A precise neural encoding of the emitted signal is crucial for functional echolocation. Among other functions, it enables distinguishing self-emitted calls and echoes from conspecific calls and echoes, and it enables coping with potential ambiguities [20–22]. The EEG signals we recorded from bats flying in place while freely echolocating allowed us to examine the brain stem's response to individual echolocation calls. In our set-up, bats produced a range of call durations while flying in the harness. We observed that iABR latencies decreased in response to shorter echolocation calls (figures 3 and 4C), consistent with findings from Luo *et al.* [23]. This faster neural response to shorter frequency-modulated (FM) calls may reflect enhanced synchrony across a broader population of neurons, facilitating the rapid auditory processing needed during the final stages of target approach (when calls become shorter).

Previous recordings of cochlear microphonics (CM) were obtained during simulated flight in a pendulum after bats had been anaesthetized and undergone surgery to place electrodes within the fluids of the inner ear [24]. Although the researchers found that the bat's ear was poorly stimulated by the intense emitted pulses, our results demonstrate that in awake, actively flying bats, self-emitted calls evoke robust ABRs, indicating that early auditory processing stages preserve a clear representation of these vocalizations despite the suggested peripheral attenuation.

A major finding of our study was the interaction between call duration and intensity with iABR amplitudes (table 1; figure 4A,B), suggesting increasing integration of acoustic information along successive auditory nuclei. For calls of similar power, signal energy scales positively with call duration (energy = power × time). Thus, longer calls might be expected to elicit larger ABR amplitudes simply because they contain more total acoustic energy. However, when the signals are FM sweeps, shorter FM sweeps stimulate a broad range of cochlear frequencies within a short time window, resulting in strong neural synchrony across afferents. This synchrony can generate a large compound ABR amplitude. Conversely, longer-duration FM calls activate cochlear regions in sequence rather than simultaneously reducing synchrony and yielding smaller summed potentials at early auditory stages. This may explain why, in response to FM echolocation calls, the positive interaction between call duration and intensity was absent in wave I—reflecting auditory-nerve activity—but became progressively stronger in waves II and III, corresponding to higher brainstem nuclei such as the superior olivary complex and inferior colliculus.

Although larger response amplitudes may reflect broader neural recruitment rather than enhanced selectivity, the higher ABR amplitudes observed for longer and more intense calls at later brainstem stages suggest that call duration is more robustly encoded in stronger calls. Correctly identifying call duration (and other properties not tested here) may assist bats in distinguishing their own calls amid a dense acoustic environment—a process particularly relevant for longer and more intense search calls. The strengthening of the duration–intensity interaction across successive ABR waves further supports the idea that later stages of the auditory brainstem engage in cumulative or integrative encoding of acoustic parameters. This temporal

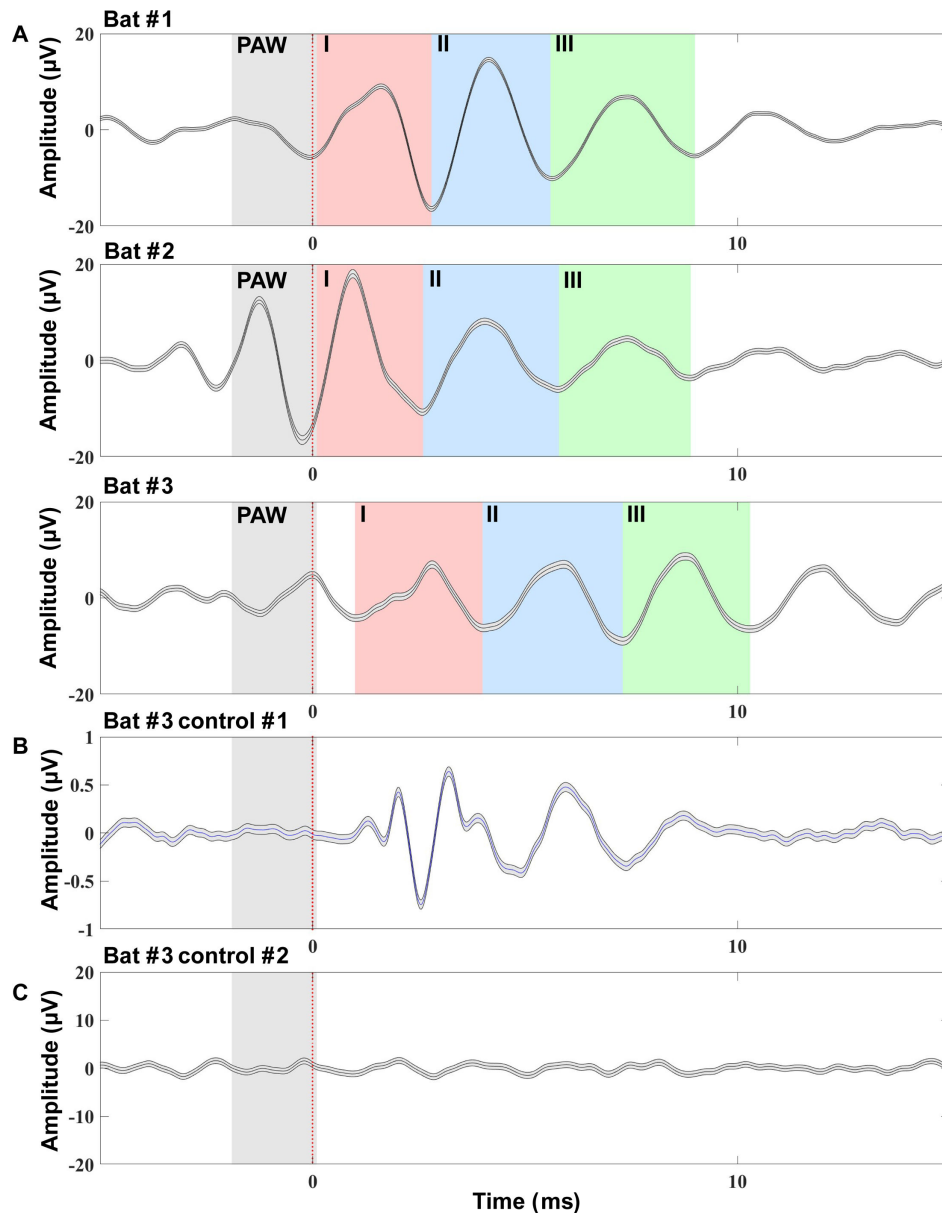


Figure 2. Average neural representation of self-generated echolocation calls. (A) Averaged EEG responses in bats #1–3 to their own echolocation calls. The vertical red line denotes the arrival of the call at the ears (time 0). The coloured background windows (red, blue and green) were defined based on the morphology of the average auditory brainstem response (ABR) waveform and constitute the search windows for waves I, II and III, respectively. An additional 2 ms long grey window was included to highlight the pre-auditory wave (PAW), which can be observed in the harness condition (A), but not in the two control conditions (B and C). Bat #3's trace shows delayed responses, potentially due to its longer call durations (1.84 ± 0.51 ms) compared to bat #1 (1.47 ± 0.41 ms) and bat #2 (0.72 ± 0.40 ms). (B) Control EEG response from bat #3 during passive listening to the playback. The first wave appears at 2.2 ms after the signal arrives at the ears. Note that the y-axis scale is different because the conditions were different (active versus passive), and the intensity of the playback was reduced compared to the natural echolocation calls (average of approx. 92 dB SPL compared with approx. 109 dB SPL at the bat's ear). The vertical red line denotes the arrival of the call at the ears (time 0). (C) Control EEG response from bat #3 while flying in the harness, with electrodes on its lower back. The vertical red line denotes the arrival of the call at the ears (time 0).

progression reinforces the interpretation that the responses we measured are auditory in nature rather than motor-related, reflecting genuine sensory processing within the ascending auditory pathway.

Previous studies have shown that auditory neurons in higher brain regions of bats including the superior colliculus and the auditory cortex are tuned to specific, often intermediate, echo intensities [8,25,26]. The intensity sensitivity that we show in lower brain regions should allow an accurate estimate of call and echo intensity, and this might facilitate this sensitivity to intermediate intensities.

We also uncovered a PAW in bats (figure 2), a phenomenon previously described in dolphins [14] and thought to be associated with the motor production of sound emissions [15]. This interpretation is consistent with prior reports of pre-vocal motor activity linked to vocal onset in freely flying bats [13].

Our observations support the idea that rapid sensory–motor coupling is a hallmark of echolocation. Brainstem encoding may facilitate faster and more efficient downstream processing, enabling the exceptionally rapid response times characteristic of bats. Free-flying bats exhibit a superfast Lombard response within approximately 20 ms of noise onset, probably mediated by brainstem-level reflex circuits [27]. They can also adjust flight and call parameters within tens of milliseconds to sudden prey-related changes, reflecting extraordinary sensory–motor agility [28]. Together, these findings suggest that early encoding

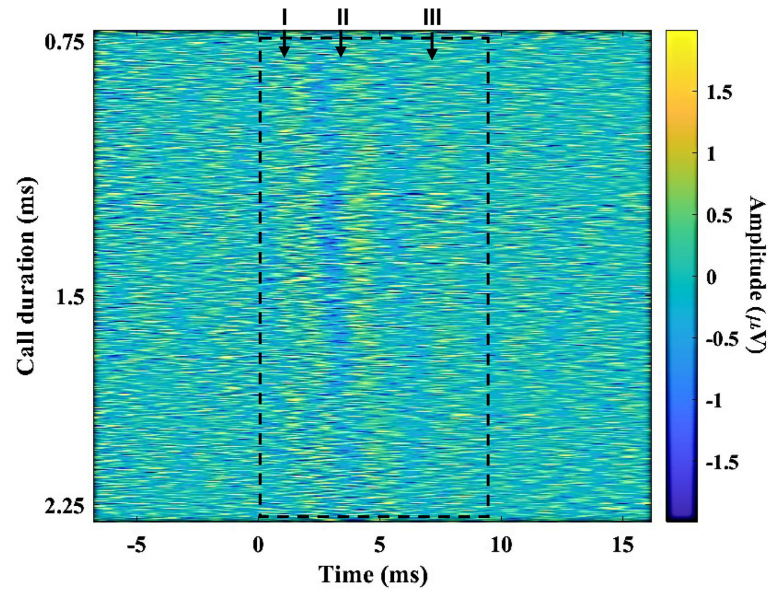


Figure 3. Single-trial iABRs in bat #1. EEG responses are sorted by echolocation call duration, from shortest (top, 0.5 ms) to longest (bottom, 3 ms). Time 0 marks the call's arrival at the ears. Waves I, II and III are marked.

of self-emitted calls at the brainstem level may contribute to rapid adaptive control during active echolocation. The average ABRs recorded in our study diverged from those previously reported in stationary big brown bats exposed to repeated FM sweeps. Specifically, our recordings did not display four rapid waves within approximately 6 ms of stimulus onset, as typically seen in anaesthetized animals [29]. Instead, we observed waves that were more temporally dispersed. This difference may be attributable to the noisier recording conditions associated with bats flying in the harness. Under these conditions, the three main waves observed in the averaged morphology may occasionally represent the merging of several smaller sub-waves, as seen in individual-response examples (see electronic supplementary material, figure S5).

Several mechanisms have been suggested for the bat brain's ability to register the emitted signal, including internal copies of motor commands (efference copies) [30,31], or internal bone conduction pathways [32]. While our data do not exclude other possibilities, they support the idea that the emitted call, as received through the bat's own auditory periphery, is encoded by the brain as early as the brainstem, despite the peripheral attenuation of self-emitted calls relative to echoes, as recorded in CM responses [24,33–35]. This aligns with the hypothesis that bats actively listen to their own vocalizations as a strategy for monitoring outgoing signals [6], allowing for precise tracking of echolocation parameters.

Overall, these findings provide new insight into how the bat auditory system processes self-generated acoustic signals in real time. By using a naturalistic, non-invasive approach that preserves active vocal behaviour, we demonstrate that the auditory brainstem tracks not only the presence of emitted signals but also their detailed acoustic properties. This opens new avenues for exploring how motor and sensory systems interact in echolocating animals.

4. Methods

(a) Animals and permits

Three adult female big brown bats (*E. fuscus*) participated in the experiment. All procedures were approved by the Institutional Animal Care and Use Committee (IACUC) of Tel Aviv University (permit number: 04-21-043). The bats were imported from the United States with all necessary permits.

(b) Preliminary experiment

(i) Acoustic stimulation

To develop the system, we first recorded ABR in passively listening, awake bats in response to repeated playback (as is standard in ABR recordings) of an echolocation call. The specific *E. fuscus* echolocation call used for playback (electronic supplementary material, figure S2) was recorded using an ultrasonic wide-band microphone (USG Electret Ultrasound Microphones—Avisoft Bioacoustics/Knowles FG). The signal was digitized at a 500 kHz sampling rate with an Avisoft A/D converter and subsequently high-pass filtered at 15 kHz and low-pass filtered at 100 kHz. The call was approximately 1 ms in duration and consisted of two harmonics centred around 35 and 70 kHz.

The acoustic signal was calibrated to approximately 100 dB SPL at the bat's ear using a calibrated GRAS 40DP 1/8" microphone (GRAS Sound & Vibration). The stimulus was presented approximately 4000 times for each of two opposite polarities—condensation and rarefaction (electronic supplementary material, figure S2B)—at a rate of approximately 14 presentations per

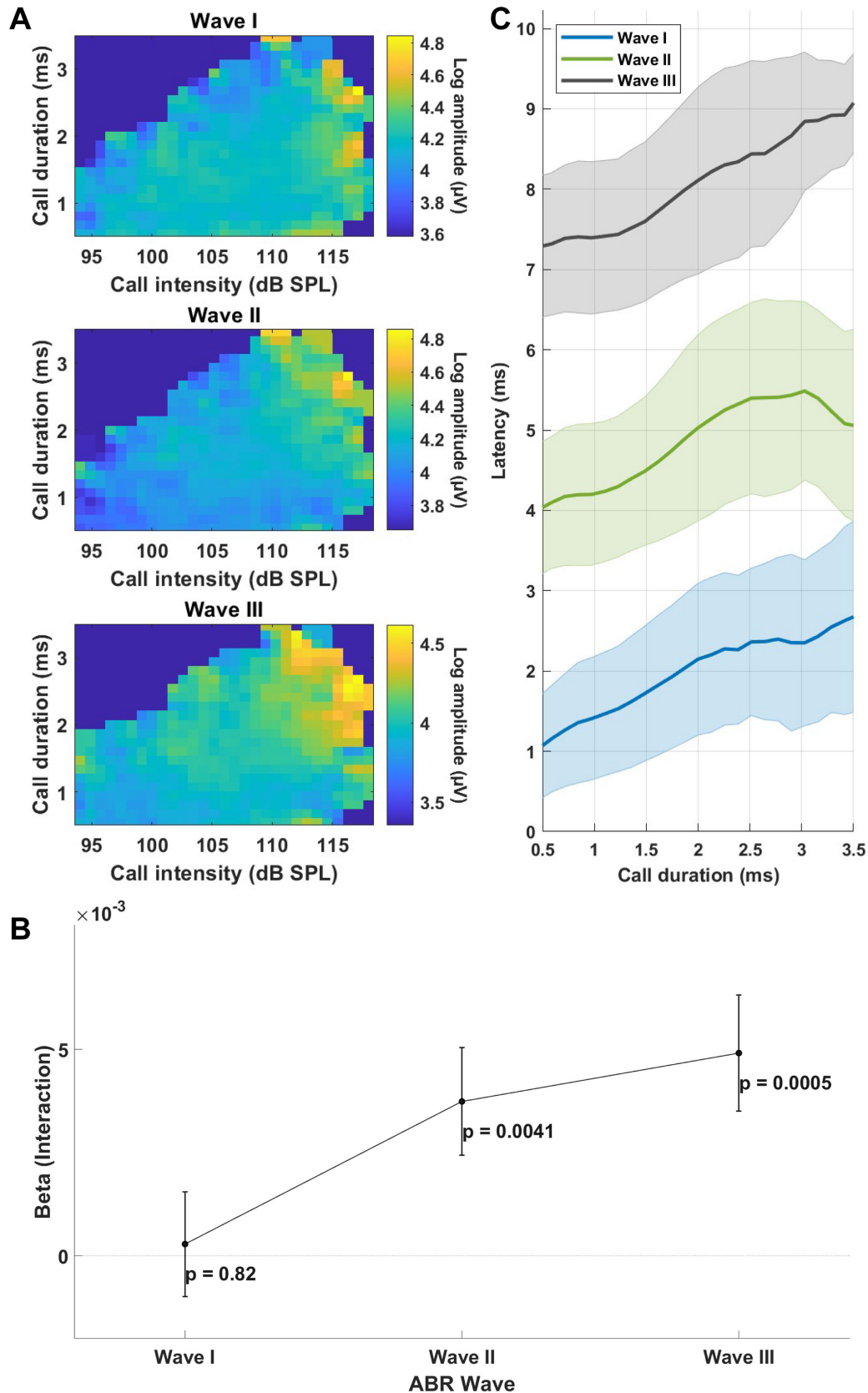


Figure 4. Echolocation acoustic properties are encoded in ABRs. (A) Heatmaps depicting average log-transformed ABR amplitude (colour bar) as a function of echolocation call intensity (x -axis) and duration (y -axis) for waves I–III. Gaussian smoothing was applied using a 3×3 pixel kernel ($\sigma = 0.7$) with symmetric boundary padding. (B) Fixed-effect estimates (β) of the interaction between call duration and intensity on the log-transformed response amplitude show a growing positive association across waves I–III, suggesting increasing integration of duration and intensity cues in later auditory processing stages. (C) Latency of waves I–III as a function of call duration (ms). Mean responses from all three bats are shown ($n = 14\,364$). Shaded areas indicate standard deviation. In a control analysis (electronic supplementary material, table S1), rise time (<0.2 ms) was included as an additional random effect to control for changes in amplitude dynamics.

second. Responses were averaged to improve the SNR [36]. To convert the stimulus from condensation to rarefaction polarity, the waveform was multiplied by -1 [37]. Alternating polarities are commonly used to eliminate stimulus artefacts [37–39] and have previously been applied in *E. fuscus* [40].

Table 1. Summary of best-fitting linear mixed-effects models ($n = 14\,364$; data collected from three bats) examining the relationships between ABR latency and log-transformed amplitude (waves I–III) and acoustic call parameters. Reported values include fixed-effect estimates (β), effect types (linear, interaction), associated p -values and AIC values. All models included random intercepts for bat identity to account for between-subject variability; amplitude models additionally incorporated EEG trial noise as a second random effect to control for recording-related variance. For wave I amplitude, a model with interaction was selected despite a slightly higher AIC ($\Delta\text{AIC} = 2$) to maintain consistency across waves. Bold p -values indicate statistical significance ($p < 0.05$).

variable	formula	random effects	AIC	predictor	effect type	β (estimate)	p -value
wave I amplitude	log_wave1_amplitude ~ dur_call * intensity_dB + (1 bat) + (1 noise)	bat ID: s.d. = 0.016 [0.005–0.050] noise: s.d. = 0.244 [0.202–0.294] residual: s.d. = 0.392 [0.388–0.397]	14 158	duration	linear	−0.096	0.48
				intensity	linear	0.0055	0.0019
				duration × intensity	interaction	0.00028	0.82
wave II amplitude	log_wave2_amplitude ~ dur_call * intensity_dB + (1 bat) + (1 noise)	bat: s.d. = 0.087 [0.038–0.198] noise: s.d. = 0.271 [0.226–0.325] residual: s.d. = 0.400 [0.395–0.405]	14 736	duration	linear	−0.41	0.0034
				intensity	linear	0.00235	0.199
				duration × intensity	interaction	0.00374	0.0041
wave III amplitude	log_wave3_amplitude ~ dur_call * intensity_dB + (1 bat) + (1 noise)	bat: s.d. = 0.110 [0.049–0.249] noise: s.d. = 0.326 [0.271–0.392] residual: s.d. = 0.432 [0.427–0.437]	16 951	duration	linear	−0.538	0.0004
				intensity	linear	−0.00041	0.837
				duration × intensity	interaction	0.00491	0.0005
wave I latency	wave1_latency ~ dur_call + intensity_dB + (1 bat)	bat ID: s.d. = 0.513 [0.230–1.142] residual: s.d. = 0.738 [0.730–0.747]	32 084	duration	linear	0.206	<0.0001
				intensity	linear	0.00588	0.0004
wave II latency	wave2_latency ~ dur_call + intensity_dB + (1 bat)	bat ID: s.d. = 0.657 [0.295–1.462] residual: s.d. = 0.790 [0.781–0.799]	34 036	duration	linear	0.237	<0.0001
				intensity	linear	0.00225	0.204
wave III latency	wave3_latency ~ dur_call + intensity_dB + (1 bat)	bat ID: s.d. = 0.609 [0.274–1.357] residual: s.d. = 0.861 [0.851–0.871]	36 486	duration	linear	0.179	<0.0001
				intensity	linear	0.00347	0.072

Auditory stimuli used in human ABR recordings typically consist of relatively low-frequency content. For example, a commonly used click stimulus contains most of its energy in the 2000–4000 Hz range [41–43]. This overlaps with the frequency range of the ABR itself, which generally spans 100–3000 Hz [37], potentially confounding the recorded response. Similarly, in bats, ABRs contain frequency components up to approximately 3000 Hz [44–46].

However, the natural echolocation calls of *E. fuscus* contain frequencies well above 3000 Hz. Combined with our observation of similar waveform responses for both condensation and rarefaction polarities within the auditory signal presentation window (electronic supplementary material, figure S3), this suggests that stimulus artefacts and ABR components can be effectively separated via appropriate filtering. Consequently, alternating polarity may not be necessary when using high-frequency auditory stimuli. This supports the feasibility of recording ABRs in response to self-emitted, high-frequency echolocation calls during flight in the harness—without polarity manipulation—while minimizing concerns about stimulus artefact contamination.

Furthermore, inclusion of random intercepts for bat identity in the harness experiment (table 1) revealed significant between-subject variability beyond the tested acoustic parameters (call intensity and duration). This indicates that individual bats exhibited consistent differences in their ABRs, even when exposed to acoustically similar calls. Such between-subject variation lends support to the assumption that the recorded ABRs reflect genuine neurophysiological processing, rather than passive transmission of acoustic properties or contamination by stimulus artefacts.

(ii) Electroencephalogram recordings

ABRs were recorded non-invasively from awake bats using AgCl/Ag tab adhesive electrodes (Bionen), trimmed to approximately 0.5×0.3 cm² and attached to three exposed wires. During electrode placement, each bat was gently restrained in a

cloth, and fur was removed from the head area using a depilatory cream (Veet Sensitive Skin, Reckitt Benckiser) applied for approximately 3 min [47]. The skin was then cleaned with 70% alcohol.

Electrodes were positioned as follows: (i) the recording electrode on the right mastoid; (ii) the reference electrode on the forehead; and (iii) the ground electrode on the left mastoid [48,49]. In an additional control recording conducted on one bat, all three electrodes were instead positioned on the lower back.

Electrodes were secured using Collodion glue (Mavidon), and a drying period of 35 min was observed before recordings began to ensure firm attachment. Following data collection, residual glue was removed using 70% alcohol.

The electrodes were connected to a custom-built differential amplifier that amplified the signals by a factor of 10 000. The amplifier included a high-pass filter at 0.159 Hz, a low-pass filter at 4.1 kHz and a selectable 50 Hz notch filter to suppress power line noise. The circuit was based on a classical AC-coupled amplifier design, similar to those described in previous studies [50–52].

To minimize electromagnetic and acoustic interference, recordings were conducted inside a Faraday cage ($55 \times 40 \times 40 \text{ cm}^3$) lined with acoustic foam. The cage was placed within a sound-attenuated room ($5.5 \times 4.5 \times 2.5 \text{ m}^3$) with anechoic acoustic foam covering the walls.

Auditory stimuli were presented through a Vifa speaker connected to an Avisoft 116 D/A converter, positioned approximately 10 cm in front of the bat. Acoustic signals were recorded using an ultrasonic microphone placed approximately 3 cm to the right of the bat and were synchronized with the EEG recordings using a National Instruments (NI) X Series data acquisition (DAQ) board. Data were collected using a custom Python script at a total sampling rate of 500 kHz (250 kHz for the EEG channel and 250 kHz for the acoustic channel). Preliminary experiment results are shown in electronic supplementary material, figure S3.

(c) Harness experiment

The custom in-house system described above was also used to record average neural responses to self-emitted echolocation calls from three *E. fuscus* bats flying in place while suspended in a 3D-printed harness (electronic supplementary material, figure S4). The harness was mounted inside the sound-attenuated Faraday cage, and an ultrasonic microphone was positioned approximately 30 cm in front of the bat, rather than approximately 3 cm to the right of the bat, as in the preliminary experiment. The amplitude was calibrated using the GRAS microphone, and all subsequent dB SPL calculations related to the harness condition were based on this calibration. Bats either flew voluntarily or were gently stimulated to fly with a light touch. Based on continuous acoustic recordings, the bats consistently emitted echolocation calls during flight. EEG signals were recorded non-invasively and synchronized with the acoustic recordings, as described in the previous section.

For one of the three bats (bat #3), two additional control recordings were conducted. (i) EEG was recorded in response to playback of echolocation sequences previously recorded from the same bat while it was flying in the harness. These sequences (approx. 1000 distinct calls, each played back approximately eight times) were presented while the bat was not placed in the harness used for flight experiments, but was stationary, restrained, awake and passively listening. (ii) EEG was recorded while the bat was flying in the harness, but with electrodes placed on the lower back.

(d) Data analysis

The raw recordings were processed in MATLAB. The EEG signal was first band-pass filtered between 300 Hz and 3000 Hz using an 18th-order Butterworth filter. In the playback experiment, to synchronize the ABR with the acoustic stimulus, we first identified the timing of the calls based on the first auditory sample that exceeded a predefined amplitude threshold (an absolute peak greater than approx. 80 dB SPL). The script then skipped 60 ms and continued searching for the next auditory signal, and so on. For each detected auditory event, a window of 10 ms pre-signal and 50 ms post-signal was extracted. Equivalent windows were cut from the filtered EEG signal, and the thousands of response windows were subsequently averaged.

Data analysis for the harness experiment followed a similar approach, with some modifications: the acoustic signal was passed through a 10 000 Hz high-pass filter to eliminate flight-related noise. The onset of the auditory signals was detected as the first sample exceeding approximately 88 dB SPL (or approx. 76 dB SPL in the first control condition, where echolocation sequences were played back to the bat while it was awake, restrained and passively listening).

For ABR analysis, calls were selected based on the following criteria: (i) calls with a peak amplitude greater than approximately 94 dB SPL (or greater than approx. 82 dB SPL for the first control); (ii) calls whose rise time—from noise level to the identified onset (88 dB SPL)—was consistent and occurred within 0.2 ms; (iii) only response windows containing a single echolocation call were included; and (iv) since EEG recordings during flight were generally noisier (probably due to electromyographic activity), windows with a maximum absolute amplitude exceeding 500 microvolts were excluded to avoid capturing clipped or noisy responses.

Time values were corrected to account for the approximately 30 cm distance between the bat and the microphone (i.e. approx. 1 ms) to reflect the actual time at which the bat heard the sound.

While it is a standard practice to average multiple responses [53–55] in order to suppress electrical noise and obtain cleaner ABR signals, recent studies have shown that when using suprathreshold stimuli, single-trial data can also be analysed effectively [15,56]. Accordingly, we analysed iABRs in the harness condition—specifically, responses evoked by single echolocation calls that varied in duration and intensity. These calls differed from those used in the preliminary experiment, in which a single signal was played repeatedly.

The call duration was calculated from the amplitude by locating the peak and then expanding backward and forward until the amplitude dropped below half of the peak amplitude. The duration was defined as the time difference between these start and end indices (converted to milliseconds using the sampling rate).

Additionally, a short rise-time window beginning 0.2 ms before onset detection was used as a criterion to select calls with similar onsets. Specifically, calls were included when their pre-window amplitudes stayed below half the threshold (82 dB SPL) up to 0.2 ms before they reached the onset detection threshold of 88 dB SPL. Moreover, we ran another control where duration was computed based on the 0.25 amplitude drop from the maximum amplitude. The results were similar to those obtained using the half-amplitude (0.5) criterion (electronic supplementary material, table S2). We examined the patterns in maximum amplitude and latency (relative to call onset) for each iABR. The total number of iABRs analysed—each representing a response to a single call emission—was 7661 for bat #1, 2837 for bat #2 and 3866 for bat #3, out of an initial pool of 12 725, 4047 and 5274 responses, respectively; low SNR epochs were excluded based on SNR values calculated from approximately 4 ms at the end of each response window. We then compared the iABR parameters to the acoustic properties of the echolocation calls that evoked them, including the calls' maximum intensity and duration. For each bat, data were extracted from the first three prominent waves of the ABR waveform. For each of the three bats, the temporal search windows corresponding to waves I, II and III were defined based on the morphology of the average ABR of that individual (see figure 2). The window boundaries were chosen to encompass the characteristic positive peaks observed in the averaged waveform, thus accounting for individual differences in response latency. Within each predefined window, a local-maximum search was performed on every single-trial iABR trace to detect the corresponding wave peak in individual responses.

(e) Statistical modeling

Separate LME models were fitted for latency and amplitude across waves I–III. Model fitting was performed in MATLAB.

For latency, candidate models included call duration and intensity as fixed effects, and a duration \times intensity interaction. All latency models included random intercepts for bat identity to account for between-subject variability.

For amplitude, candidate models included both raw and log-transformed amplitude values ($\log[x + 1]$), with combinations of duration, intensity and their interaction as fixed effects. All amplitude models included random intercepts for both bat identity and EEG noise group, the latter capturing session-level variability in noise and modelled as a categorical random effect to reflect its discrete nature. This specification significantly improved model performance, as indicated by lower Akaike information criterion (AIC) values.

The final best-fitting models were selected based on the lowest AIC for each wave.

For wave I amplitude, although the lowest-AIC model did not include an interaction, a model with the interaction term ($\Delta\text{AIC} = 2$) was selected to maintain consistency across waves.

Model residuals were examined for violations of model assumptions. Latency models exhibited banded residual patterns, consistent with the quantized (discrete) nature of neural timing rather than model misfit. Amplitude models showed symmetrical and homoscedastic residuals following log transformation.

Details of the best-fitting models, including fixed effects and AIC values, are presented in table 1.

Ethics. Three adult female big brown bats (*Eptesicus fuscus*) participated in the experiment. All procedures were approved by the Institutional Animal Care and Use Committee (IACUC) of Tel Aviv University (permit number: 04-21-043). The bats were imported from the United States with all necessary permits.

Data accessibility. The dataset is publicly available at Dryad [57]

Supplementary material is available online [58].

Declaration of AI use. AI-assisted technologies were used for language editing/proofreading and for coding and statistical input.

Authors' contributions. Y.C.T.: data curation, formal analysis, investigation, methodology, software, visualization, writing—original draft, writing—review and editing; A.S.: methodology, writing—original draft; A.L.: methodology; Y.Y.: conceptualization, funding acquisition, investigation, methodology, project administration, resources, supervision, validation, writing—original draft, writing—review and editing.

All authors gave final approval for publication and agreed to be held accountable for the work performed therein.

Conflict of interest declaration. We declare we have no competing interests.

Funding. No funding has been received for this article.

Acknowledgements. We gratefully acknowledge the following contributors: Mor Taub for assistance with 3D printing of the harness and for generating the schematic in figure 1A; Dr Arjan Boonman for assistance with acoustics consultations and 3D printing of the harness; Omer Mazar for help with recording the echolocation call presented in electronic supplementary material, figure S2 and for coding consultations; Dr Maya Weinberg for veterinary consultations; Dr Ofri Eitan and Nir Dgani for additional support with 3D printing of the harness; Yoni Amit for writing the original Python script used to collect the raw data; Xing Chen for setting up our Python environment; Eithan Tarnovsky for constructing our harness holder; and Naomi Paz for proofreading earlier versions of the manuscript.

References

1. de Framond L, Reininger V, Goerlitz HR. 2023 Temperate bats may alter calls to partially compensate for weather-induced changes in detection distance. *J. Acoust. Soc. Am.* **153**, 2867. (doi:10.1121/10.0019359)
2. Griffin DR. 1958 *Listening in the dark: the acoustic orientation of bats and men*. New Haven, CT: Yale University Press.
3. Chiu C, Xian W, Moss CF. 2009 Adaptive echolocation behavior in bats for the analysis of auditory scenes. *J. Exp. Biol.* **212**, 9. (doi:10.1242/jeb.027045)

4. Diebold CA, Salles A, Moss CF. 2020 Adaptive echolocation and flight behaviors in bats can inspire technology innovations for sonar tracking and interception. *Sensors* **20**, 2958. (doi:10.3390/s20102958)
5. Fenton MB. 2003 Eavesdropping on the echolocation and social calls of bats. *Mammal Rev.* **33**, 3. (doi:10.1046/j.1365-2907.2003.00019.x)
6. Simmons JA. 1979 Perception of echo phase information in bat sonar. *Science* **204**, 1336–1338. (doi:10.1126/science.451543)
7. Jones G. 2005 Echolocation. *Curr. Biol.* **15**, R484–8. (doi:10.1016/j.cub.2005.06.051)
8. Grinnell AD. 1963 The neurophysiology of audition in bats: intensity and frequency parameters. *J. Physiol.* **167**, 1. (doi:10.1113/jphysiol.1963.sp007132)
9. Suga N. 1969 Echo-location and evoked potentials of bats after ablation of inferior colliculus. *J. Physiol.* **203**, 707–728. (doi:10.1113/jphysiol.1969.sp008888)
10. Osanai H, Tateno T. 2016 Neural response differences in the rat primary auditory cortex under anesthesia with ketamine versus the mixture of medetomidine, midazolam and butorphanol. *Hear. Res.* **339**, 69–79. (doi:10.1016/j.heares.2016.06.012)
11. Cui J, Zhu B, Fang G, Smith E, Brauth SE, Tang Y. 2017 Effect of the level of anesthesia on the auditory brainstem response in the emei music frog (*Babina daunchina*). *PLoS One* **12**, e0169449. (doi:10.1371/journal.pone.0169449)
12. Simmons AM, Tuninetti A, Yeoh BM, Simmons JA. 2022 Non-invasive auditory brainstem responses to FM sweeps in awake big brown bats. *J. Comp. Physiol.* **208**, 505–516. (doi:10.1007/s00359-022-01559-w)
13. Sinha SR, Moss CF. 2007 Vocal premotor activity in the superior colliculus. *J. Neurosci.* **27**, 98–110. (doi:10.1523/JNEUROSCI.2683-06.2007)
14. Finneran JJ, Mulsow J, Jones R, Houser DS, Accomando AW, Ridgway SH. 2017 Non-auditory, electrophysiological potentials preceding biosonar click production in bottlenose dolphins. *J. Acoust. Soc. Am.* **142**, 2691–2691. (doi:10.1121/1.5014818)
15. Finneran JJ, Mulsow J, Jones R, Houser DS, Accomando AW, Ridgway SH. 2018 Non-auditory, electrophysiological potentials preceding dolphin biosonar click production. *J. Comp. Physiol.* **204**, 271–283. (doi:10.1007/s00359-017-1234-0)
16. Griffin DR. 1953 Bat sounds under natural conditions, with evidence for echolocation of insect prey. *J. Exp. Zool.* **123**, 435–465. (doi:10.1002/jez.1401230304)
17. Simmons JA, Fenton MB, O'Farrell MJ. 1979 Echolocation and pursuit of prey by bats. *Science* **203**, 16–21. (doi:10.1126/science.758674)
18. Surlykke A, Moss CF. 2000 Echolocation behavior of big brown bats, *Eptesicus fuscus*, in the field and the laboratory. *J. Acoust. Soc. Am.* **108**, 5. (doi:10.1121/1.1315295)
19. Nachtigall PE, Schuller G. 2014 Hearing during echolocation in whales and bats. *Biosonar* 143–167. (doi:10.1007/978-1-4614-9146-0_5)
20. Goldshtein A *et al.* 2025 Onboard recordings reveal how bats maneuver under severe acoustic interference. *Proc. Natl Acad. Sci. USA* **122**, e2407810122. (doi:10.1073/pnas.2407810122)
21. Mazar O, Yovel Y. 2020 A sensorimotor model shows why a spectral jamming avoidance response does not help bats deal with jamming. *eLife* **9**, e55539. (doi:10.7554/eLife.55539)
22. Melcón ML, Yovel Y, Denzinger A, Schnitzler HU. 2011 How greater mouse-eared bats deal with ambiguous echoic scenes. *J. Comp. Physiol. A* **197**, 505–514. (doi:10.1007/s00359-010-0563-z)
23. Luo J, Macias S, Ness TV, Einevoll GT, Zhang K, Moss CF. 2018 Neural timing of stimulus events with microsecond precision. *PLoS Biol.* **16**, e2006422. (doi:10.1371/journal.pbio.2006422)
24. Henson Jr OW. 1987 Biosonar imaging of insects by *Pteronotus p. parnellii*, the mustached bat. *Nat. Geograph. Res* **3**, 82–101.
25. Macias S, Hechavarría JC, Cobo A, Mora EC. 2014 Narrow sound pressure level tuning in the auditory cortex of the bats *Molossus molossus* and *Macrotus waterhousii*. *Hear. Res.* **309**, 36–43. (doi:10.1016/j.heares.2013.11.004)
26. Macias S, Mora EC, Hechavarría JC, Kössl M. 2016 Echo-level compensation and delay tuning in the auditory cortex of the mustached bat. *Eur. J. Neurosci.* **43**, 1647–1660. (doi:10.1111/ejn.13244)
27. Pedersen MB *et al.* 2024 Superfast Lombard response in free-flying, echolocating bats. *Curr. Biol.* **34**, 2509–2516. (doi:10.1016/j.cub.2024.04.048)
28. Geberl C, Brinkløv S, Wiegrebe L, Surlykke A. 2015 Fast sensory-motor reactions in echolocating bats to sudden changes during the final buzz and prey intercept. *Proc. Natl Acad. Sci. USA* **112**, 4122–4127. (doi:10.1073/pnas.1424457112)
29. Burkard R, Moss CF. 1994 The brain-stem auditory-evoked response in the big brown bat (*Eptesicus fuscus*) to clicks and frequency-modulated sweeps. *J. Acoust. Soc. Am.* **96**, 2. (doi:10.1121/1.410318)
30. Chagnaud BP, Simmers J, Straka H. 2012 Predictability of visual perturbation during locomotion: implications for corrective efference copy signaling. *Biol. Cybern.* **106**, 669–679. (doi:10.1007/s00422-012-0528-0)
31. Li S, Zhu H, Tian X. 2020 Corollary discharge versus efference copy: distinct neural signals in speech preparation differentially modulate auditory responses. *Cereb. Cortex* **30**, 5806–5820. (doi:10.1093/cercor/bhaa154)
32. Veselka N, McErlain DD, Holdsworth DW, Eger JL, Chhem RK, Mason MJ, Brain KL, Faure PA, Fenton MB. 2010 A bony connection signals laryngeal echolocation in bats. *Nature* **463**, 939–942. (doi:10.1038/nature08737)
33. Henson OW, Pollak GD, Kobler JB, Henson MM, Goldman LJ. 1982 Cochlear microphonic potentials elicited by biosonar signals in flying bats, *Pteronotus p. parnellii*. *Hear. Res.* **7**, 127–147. (doi:10.1016/0378-5955(82)90010-7)
34. Henson Jr OW, Keating AW, Henson MM. 1989 Evoked potential correlates of echolocation in the mustached bat, *Pteronotus p. parnellii*. *Hear. Res.* **38**, 213–219. (doi:10.1016/0378-5955(89)90066-x)
35. Henson OW, Koplak PA, Keating AW, Huffman RF, Henson MM. 1990 Cochlear resonance in the mustached bat: behavioral adaptations. *Hear. Res.* **50**, 259–273. (doi:10.1016/0378-5955(90)90050-y)
36. Jamal FN, Arafat Dzulqarnain AA, Shahrudin FA, Marzuki MN. 2021 Test-retest reliability of level-specific CE-chirp auditory brainstem response in normal-hearing adults. *J. Audiol. Otol.* **25**, 14–21. (doi:10.7874/jao.2020.00073)
37. Skoe E, Kraus N. 2010 Auditory brain stem response to complex sounds: a tutorial. *Ear Hear.* **31**, 302–324. (doi:10.1097/AUD.0b013e3181c8b272)
38. da Silva Ormundo D, Lewis DR. 2021 Auditory brainstem response with click and CE-Chirp level specific stimuli in hearing infants. *Int. J. Pediatr. Otorhinolaryngol.* **147**, 110819. (doi:10.1016/j.ijporl.2021.110819)
39. Jiang Y, Samuel OW, Asogbon MG, Chen S, Li G. 2021 Towards optimal selection of stimuli polarity method for effective evoking auditory brainstem responses. *J. Integr. Neurosci.* **20**, 297–305. (doi:10.31083/jjin2002029)
40. Weinberg MM, Retta NA, Schrode KM, Screven LA, Peterson JL, Moss CF, Sterbing S, Lauer AM. 2021 Deafness in an auditory specialist, the big brown bat (*Eptesicus fuscus*). *Hear. Res.* **412**, 108377. (doi:10.1016/j.heares.2021.108377)
41. Gorga MP, Johnson TA, Kaminski JR, Beauchaine KL, Garner CA, Neely ST. 2006 Using a combination of click- and tone burst-evoked auditory brain stem response measurements to estimate pure-tone thresholds. *Ear Hear.* **27**, 60–74. (doi:10.1097/01.aud.0000194511.14740.9c)

42. Mourtzouchos K, Riga M, Cebulla M, Danielides V, Naxakis S. 2018 Comparison of click auditory brainstem response and chirp auditory steady-state response thresholds in children. *Int. J. Pediatr. Otorhinolaryngol.* **112**, 91–96. (doi:10.1016/j.ijporl.2018.06.037)
43. Picton TW, Durieux-Smith A, Moran LM. 1994 Recording auditory brainstem responses from infants. *Int. J. Pediatr. Otorhinolaryngol.* **28**, 93–110. (doi:10.1016/0165-5876(94)90001-9)
44. Furuyama T, Hase K, Hiryu S, Kobayasi KI. 2018 Hearing sensitivity evaluated by the auditory brainstem response in *Miniopterus fuliginosus*. *J. Acoust. Soc. Am.* **144**, EL436–EL440. (doi:10.1121/1.5079904)
45. Linnenschmidt M, Wiegrebe L. 2019 Ontogeny of auditory brainstem responses in the bat, *Phyllostomus discolor*. *Hear. Res.* **373**, 85–95. (doi:10.1016/j.heares.2018.12.010)
46. Wetekam J, Hechavarría J, López-Jury L, Kössl M. 2022 Correlates of deviance detection in auditory brainstem responses of bats. *Eur. J. Neurosci.* **55**, 1601–1613. (doi:10.1111/ejn.15527)
47. Cvikel N, Levin E, Hurme E, Borissov I, Boonman A, Amichai E, Yovel Y. 2015 On-board recordings reveal no jamming avoidance in wild bats. *Proc. R. Soc. B* **282**, 20142274. (doi:10.1098/rspb.2014.2274)
48. Hunter LL, Blankenship CM, Gunter RG, Keefe DH, Feeney MP, Brown DK, Barock K. 2018 Cochlear microphonic and summing potential responses from click-evoked auditory brain stem responses in high-risk and normal infants. *J. Am. Acad. Audiol.* **29**, 427–442. (doi:10.3766/jaaa.17085)
49. Sanyelbhaa Talaat H, Kabel AH, Samy H, Elbadry M. 2009 Prevalence of auditory neuropathy (AN) among infants and young children with severe to profound hearing loss. *Int. J. Pediatr. Otorhinolaryngol.* **73**, 937–939. (doi:10.1016/j.ijporl.2009.03.009)
50. Land BR, Wyttenbach RA, Johnson BR. 2001 Tools for physiology labs: an inexpensive high-performance amplifier and electrode for extracellular recording. *J. Neurosci. Methods* **106**, 47–55. (doi:10.1016/s0165-0270(01)00328-4)
51. Matsuzaka Y, Ichihara T, Abe T, Mushiake H. 2012 Bio-amplifier with driven shield inputs to reduce electrical noise and its application to laboratory teaching of electrophysiology. *J. Undergrad. Neurosci. Educ.* **10**, A118–24.
52. Spence AJ, Neeves KB, Murphy D, Sponberg S, Land BR, Hoy RR, Isaacson MS. 2007 Flexible multielectrodes can resolve multiple muscles in an insect appendage. *J. Neurosci. Methods* **159**, 116–124. (doi:10.1016/j.jneumeth.2006.07.002)
53. Chandrasekaran B, Kraus N. 2010 The scalp-recorded brainstem response to speech: neural origins and plasticity. *Psychophysiology* **47**, 236–246. (doi:10.1111/j.1469-8986.2009.00928.x)
54. Don M, Elberling C. 1994 Evaluating residual background noise in human auditory brain-stem responses. *J. Acoust. Soc. Am.* **96**, 5. (doi:10.1121/1.411281)
55. Supin AY, Popov VV. 2007 Improved techniques of evoked-potential audiometry in odontocetes. *Aquat. Mamm.* **33**, 14–23. (doi:10.1578/am.33.1.2007.14)
56. McClaskey CM, Panganiban CH, Noble KV, Dias JW, Lang H, Harris KC. 2020 A multi-metric approach to characterizing mouse peripheral auditory nerve function using the auditory brainstem response. *J. Neurosci. Methods* **346**, 108937. (doi:10.1016/j.jneumeth.2020.108937)
57. Tarnovsky YC, Sheinin A, Laufer A, Yovel Y. 2026 In-flight neural EEG representation of echolocation in bats. Dryad Digital Repository. (doi:10.5061/dryad.dz08kps9w)
58. Tarnovsky YC, Sheinin A, Laufer A, Yovel Y. 2026 Supplementary material from: In-flight brainstem responses highlight the encoding of self-emitted echolocation calls in bats. Figshare. (doi:10.6084/m9.figshare.c.8259589)